3. METHODS[1]

Shipboard Scientific Party[2]

INTRODUCTION

In this chapter, we have assembled information that will help the reader understand the observations on which our preliminary conclusions are based and also help the interested investigator select samples for further analysis. This information concerns only shipboard operations and analyses described in the transect reports in the *Initial Reports* volume of the Leg 168 *Proceedings of the Ocean Drilling Program.*

The separate sections of the transect chapters were written by the shipboard scientific specialists for each scientific discipline (see "Participants Aboard the JOIDES Resolution for Leg 168" at the front of this volume).

Because of geologic similarities between closely spaced sites, the results of drilling at each site on Leg 168 were grouped into three transect chapters, rather than individual site chapters. This is described in the "Introduction and Summary" chapter (this volume).

Curatorial Procedures and Core Handling

Standard procedures were followed on Leg 168 for determining depths in hole, numbering of sites, holes, cores, and sections, and curation of the cores (see, for example, the Leg 159 ODP *Initial Reports* volume). Any nonroutine sampling or core analysis procedures are described in the following sections.

LITHOSTRATIGRAPHY

Sediments

Visual Core Descriptions

We followed normal ODP procedures for recording sedimentologic information on visual core description (VCD) forms, on a section-by-section basis (Mazzullo and Graham, 1988). Textural subdivisions for siliciclastic sediments and the classification scheme for siliciclastic lithologies follow Mazzullo et al. (1988). The "Graphic Lithology" column on each form shows all intervals that are at least 10 cm thick. Combined graphic patterns are used to indicate interbeds less than 10 cm in thickness. Figure 1 displays the graphic patterns for all lithologies encountered during Leg 168, together with symbols for internal sedimentary structures and symbols for core disturbance in both soft sediment and indurated rock. Sediment color was measured at 10-cm intervals on the working half of each core using a Minolta CM-2002 Spectrophotometer. The specifics of this system were described by Schneider et al. (1995). Digital color data are on CD-ROM in the back pocket of this volume (see Table 1). The "Samples" column on core description forms indicates the positions and types of whole-round samples and samples taken from each core for shipboard analyses. The abbreviations for these samples are as follows: IW = interstitial water; PP = physical properties; S = smear slide; and WR = whole-round samples.

[1]Davis, E.E., Fisher, A.T., Firth, J.V., et al., 1997. *Proc. ODP, Init. Repts,* 168: College Station, TX (Ocean Drilling Program).

[2]Shipboard Scientific Party is given in the list preceding the Table of Contents.

Smear Slides

The results of semiquantitative smear-slide analyses are tabulated and available on CD-ROM (back pocket). Visual percentage estimates for each constituent are grouped into the following categories: D = dominant (>50%); A = abundant (25%–50%); C = common (10%–25%); M = minor (5%–10%); R = rare (1%–5%); T = trace (<1%). In the "Lithology" column, "D" indicates that the sample is representative of the dominant lithology of the core, and "M" indicates a minor component. The mineral abbreviations used in the "Other" column under mineral constituents are as follows: An = anhydrite; Ar = aragonite; Ep = epidote; Ru = rutile; and To = tourmaline. These minerals were detected in trace amounts only.

X-ray Diffraction

Routine samples for shipboard X-ray diffraction (XRD) analysis were taken from approximately every other section of each core, and most were located adjacent to physical properties and carbonate samples. Samples were freeze dried, crushed either by hand or with a ball mill, and mounted as random bulk powders. The X-ray laboratory aboard the *JOIDES Resolution* is equipped with a Philips PW-1729 X-ray generator and a Philips PW-1710/00 diffraction control unit with a PW-1775 35-port automatic sample changer. Machine settings for all standards were as follows: generator = 40 kV and 35 mA; tube anode = Cu; wavelength = 1.54056 Å ($CuK_{\alpha 1}$) and 1.54439 Å ($CuK_{\alpha 2}$); intensity ratio = 0.5; focus = fine; irradiated length = 12 mm; divergence slit = automatic; receiving slit = 0.2 mm; step size = 0.02˚2θ; count time per step = 1 s; scanning rate = 4˚2θ/min; ratemeter constant = 0.2 s; spinner = off; monochronometer = on; scan = step; and scanning range = from 2˚2θ to 70˚2θ.

The software used for XRD data reduction was MacDiff 3.0.6c, a shareware application for Macintosh computers that supports routine measurement of peak intensity and peak area (see CD-ROM, back pocket, for diffractograms, peak measurements, and digital data files). The method of Fisher and Underwood (1995) was employed to determine semiquantitative relative abundances of minerals. This mathematical technique uses matrix singular value decomposition to solve for reliable normalization factors. Calibration depends upon known mixtures of mineral standards that are appropriate matches for the indigenous sediments, and the resulting normalization factors are specific to the combination of XRD hardware and software. During Leg 168, seven minerals (or mineral groups) were chosen for the standard mixtures: smectite (Ca montmorillonite); mica (combination of crystalline muscovite + illite); chlorite; quartz; total feldspar (combination of oligoclase + orthoclase); calcite (Iceland spar); and pyrite. Amphiboles were excluded because preliminary qualitative estimates indicated only small variations (2%–6%) throughout the sampled sections. Pyrite, though minor in abundance, was included because of its potential as an indicator of sediment diagenesis.

Figure 2 shows the positions and angular ranges of all peaks used in quantitative analysis. The numerical technique of Fisher and Underwood (1995) allows one to assign either positive or negative normalization factors to relate each indicator mineral to each target phase (Table 2). Normalization factors for all shipboard analyses were derived from 11 mixtures of mineral standards, each of which

was split and analyzed five times. Differences between measured weight percentages for each mineral in the standard mixtures and their respective average calculated weight percentages derived from the XRD data are less than 5% (Table 3), and the average error for all minerals is 0.8% (see CD-ROM, back pocket, for additional data). We also tested the validity of a model in which all normalization factors must be positive in sign, but this approach resulted in a weaker match between calculated and measured weight percentages of the mineral standards. A separate set of normalization factors was generated for samples analyzed at the University of Lille after Leg 168 ended. These factors were used to calculated relative mineral abundances of samples from Sites 1030, 1031, and 1032 (Table 2), and they are based on analyses of splits of the 11 shipboard mixtures of mineral standards.

Sixteen clay-sized fractions from Site 1027 were analyzed in additional detail. The previously crushed bulk-powder samples were mixed with nanopure water and exposed to a sonic dismembrator for 5 min to enhance disaggregation and suspension. After clay minerals flocculated, centrifugation at 2500 rpm was followed by more mixing with nanopure water. Suspensions then were centrifuged at 1000 rpm for 5 min to separate the <2-µm fraction, which was dropped onto glass slides to produce oriented aggregates. X-ray diffraction parameters and data processing for the oriented specimens followed procedures for bulk-powder X-ray analyses, except that the scanning range was limited between 2°2θ and 40°2θ. In addition, the clay-sized samples were saturated with ethylene glycol for 12 hr and reanalyzed to help identify expandable clay minerals.

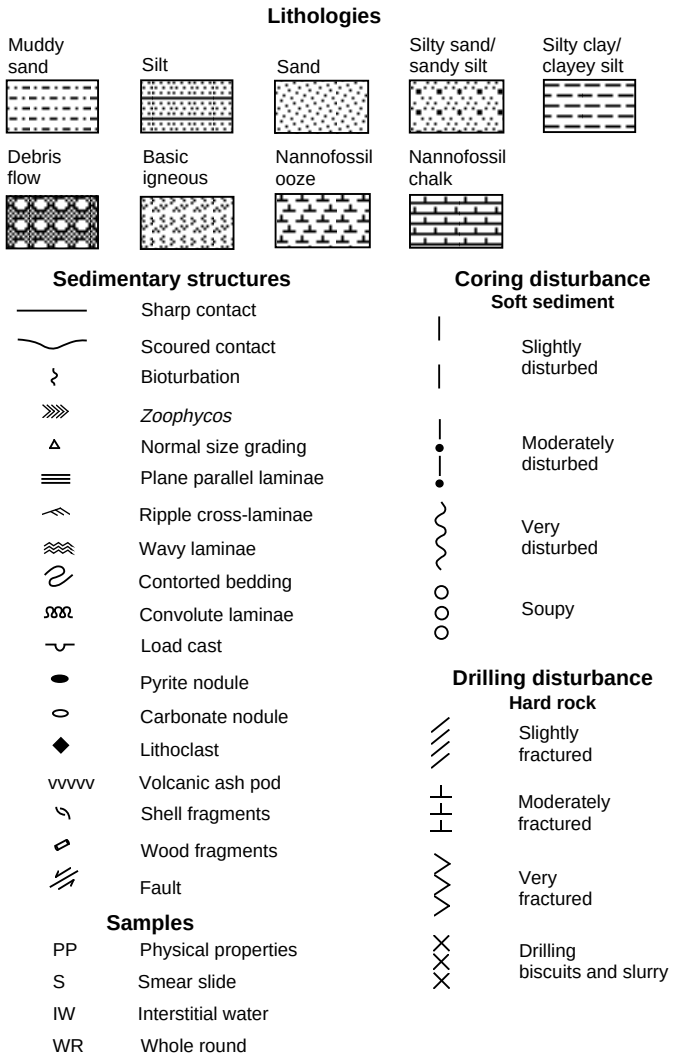

Figure 1. Graphic patterns used on core description forms to indicate lithologies encountered during Leg 168. Also shown are symbols for sedimentary structures, samples, and coring/drilling disturbance in soft sediment and hard sedimentary rock.

Basalts

Visual Core Descriptions

All igneous core descriptions completed during Leg 168 were archived electronically using a modified version of the VCD form developed during previous ODP legs (e.g., Shipboard Scientific Party, 1992a, 1993a, 1993b, and 1995a). These forms provide a graphical representation of the archive half of the core, as well as summarizing the primary magmatic and secondary alteration characteristics, along with any structural features present (Fig. 3A–D). All shipboard analyses carried out on the cores have also been listed on the VCD forms (Fig. 3C).

When describing and assigning a name to the rock sequences, cores were subdivided into lithologic units based upon changes in mineralogy, texture, grain size, composition, and the occurrence of chilled margins, with the type of data recorded similar to that in previous *Initial Reports* volumes (e.g., Shipboard Scientific Party, 1992a, 1992b, and 1993b). Unit designations for the basement lithologies are expressed using Arabic numerals (e.g., 1, 2, 3...), in contrast to the Roman numerals used to designate sedimentary units. Subunits in the basement core are denoted by lowercase letters.

Igneous Petrology

All macroscopic and microscopic descriptions of the core were logged (for a full discussion, see Shipboard Scientific Party, 1993b, 1995a) and are available on CD-ROM (back pocket). Appendixes include hand-specimen descriptions (LITHLOG), primary mineralogy (MINLOG), secondary alteration (ALTNLOG), and the presence of veins and fractures (VEINLOG) (see Appendixes A–D and thin-section descriptions, all on CD-ROM, back pocket).

Classification of Rock Types and Textures

All rocks were divided into porphyritic, aphanitic, and phaneritic groups; aphanitic rocks were subdivided into glassy, aphyric, and phyric subgroups based upon their phenocryst abundance, whereas

Table 1. Lithostratigraphic and related data files and figures on CD-ROM (back pocket).

1.	Color photospectrometer data in unprocessed ASCII files
2.	Munsell codes and representative spectral-intensity data from 430-, 550-, and 670-nm bands
3.	Plots of representative color-band intensities vs. depth
4.	Depths and thicknesses of turbidites
5.	Peak areas and peak intensities for bulk-powder X-ray diffraction analyses
6.	Relative mineral percentages calculated from X-ray diffraction data
7.	X-ray diffractograms from bulk-powder analyses
8.	X-ray diffraction peak area and peak intensities from analyses of standard mineral mixtures
9.	X-ray diffractograms from analyses of standard mineral mixtures
10.	Carbonate content from coulometric analyses

phaneritic rocks were defined as fine, medium, and coarse grained (Table 4). At the microscopic scale, rock textures were defined according to the degree of crystallinity (Table 4), with all other textural terms used based on definitions in McKenzie et al. (1982). Textural features within glass-rich zones were described using the definitions in the Leg 147 *Initial Reports* volume (Shipboard Scientific Party, 1993b) and are summarized in Figure 4. All classification and textural data are recorded in MINLOG and LITHLOG.

The modal abundances of all primary magmatic and secondary phases were calculated by point counting (based on 500 counts per section). These data, along with mineral grain size ranges and morphology, were recorded in MINLOG and ALTNLOG. All fractures and hydrothermal veins were logged on VEINLOG following the procedure established in previous *Initial Reports* volumes (e.g., Shipboard Scientific Party, 1989, 1992b, 1995a).

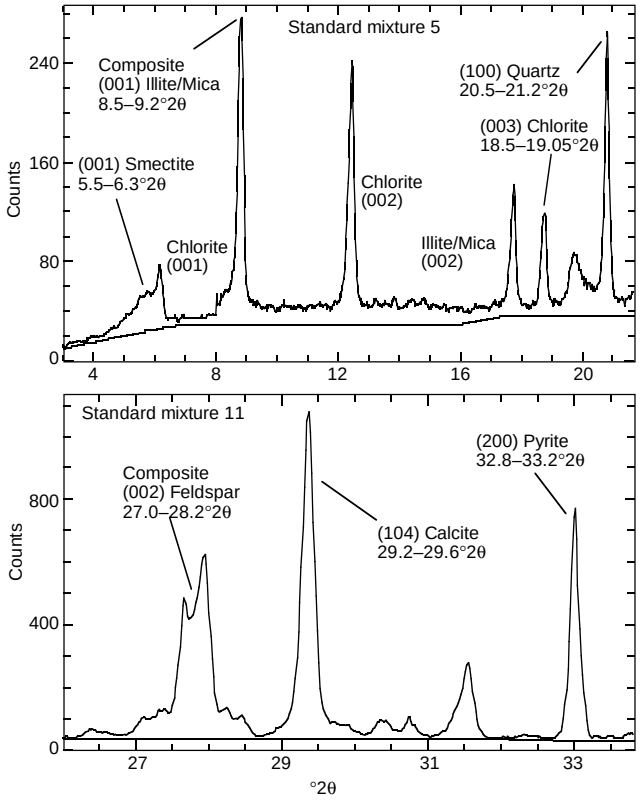

Figure 2. Examples of X-ray diffractograms showing ranges of °2θ used to calculate peak areas for minerals in both standard mixtures and natural samples.

Geochemical Analysis

X-ray Fluorescence Analysis

Representative samples of the various lithologies logged during Leg 168 were selected for major oxide analysis by X-ray fluorescence (XRF) on a fully automated wavelength-dispersive ARL8420+ system with a 3-kW generator and Rh anode X-ray tube. No trace element analyses were conducted because of technical difficulties. Table 5 summarizes the major elements analyzed along with the operating conditions. Major element analyses were made on fused glass disks (see Shipboard Scientific Party, 1993b, for a full discussion), with minor modifications made to the procedural methods during the leg. The change in major element analysis methods arose because of variations in the flux characteristics used during this leg ("Flux VI"—Spectroflux 105 from Johnson Mathey, containing 47% lithium tetraborate, 36.7% lithium carbonate, and 16.3% lanthanum oxide) compared with those used during previous legs ("Fluxes I–V"—#FF28-10 from Spex, containing 80% lithium tetraborate and 20% lanthanum oxide). Initial problems were encountered when trying to make fused glass beads following the procedures used for Fluxes I–V (see previous ODP *Initial Reports* volumes for a full discussion of this method (e.g., Shipboard Scientific Party, 1992b, 1993b). A new sample preparation method was therefore developed following the procedure outlined in Harvey et al. (1973), using a 6:1 flux to rock powder dilution with a fusion temperature of 1020°C (with a minimum of 950°C) for approximately 4–6 min (depending on the rock type). Before being added to the pre-ignited rock powder, the flux was dried at 500°C. The glass beads were made using an NT-2100 bead sampler, with 30 µL of releasing agent added to the flux/rock powder mixture. The molten glass bead was then left to cool in a $Pt_{95}Au_5$ mold for 35–40 min. Because all powders were ignited before weighing, all analyses were reported on an anhydrous basis, and all iron values were reported as ferric iron (i.e., Fe_2O_3*).

Fused beads, using the procedure outlined above, were made for the 14 standards (a mixture of internal ODP standards and international standards) listed in Table 6. These were used to calibrate the XRF spectrometer before running any unknown samples. Reported analyses for Leg 168 standards agree within 5% of the recommended values of Govindaraju (1989). Internal calibration checks were periodically made during the cruise to check for analytical precision and

Table 2. Normalization factors for Leg 168 bulk-powder samples, based on XRD peak areas and determined with matrix singular value decomposition using 11 standard mixtures.

Indicator mineral	Target Mineral: Smectite	Mica	Chlorite	Quartz	Feldspar	Calcite	Pyrite
Analyses on JOIDES Resolution (Sites 1023, 1024, 1025, 1026, 1027, 1028, and 1029)							
Smectite	1.0173×10^{-2}	-5.8804×10^{-4}	9.9315×10^{-4}	6.9618×10^{-5}	-8.3561×10^{-4}	-5.4315×10^{-4}	1.7237×10^{-4}
Mica	1.3897×10^{-4}	5.4416×10^{-3}	4.4031×10^{-4}	-5.1781×10^{-5}	-2.9043×10^{-4}	1.0912×10^{-4}	8.2766×10^{-5}
Chlorite	-3.5065×10^{-4}	9.1147×10^{-4}	7.5421×10^{-3}	-6.1976×10^{-4}	6.0902×10^{-4}	-2.3493×10^{-5}	-9.3392×10^{-5}
Quartz	-6.6648×10^{-4}	-3.5254×10^{-4}	-3.0693×10^{-4}	6.7525×10^{-3}	-1.0694×10^{-4}	-1.2632×10^{-4}	-3.2967×10^{-5}
Feldspar	-2.1271×10^{-4}	-2.3454×10^{-4}	-1.0482×10^{-4}	-5.1204×10^{-7}	2.0603×10^{-3}	-9.3009×10^{-6}	-1.9188×10^{-5}
Calcite	-2.5924×10^{-5}	-5.1167×10^{-5}	-7.0213×10^{-5}	3.2307×10^{-6}	3.8914×10^{-7}	1.3038×10^{-3}	5.4327×10^{-6}
Pyrite	1.4139×10^{-3}	1.3539×10^{-4}	-1.2855×10^{-3}	1.1382×10^{-3}	1.2270×10^{-3}	1.6355×10^{-4}	6.9023×10^{-3}
Analyses at Universite de Lille (Sites 1030, 1031, and 1032)							
Smectite	4.9905×10^{-3}	-8.9431×10^{-5}	8.1664×10^{-4}	-1.9962×10^{-4}	-2.4675×10^{-4}	-1.9726×10^{-4}	-2.2098×10^{-4}
Mica	6.9599×10^{-5}	2.5020×10^{-3}	1.8257×10^{-4}	-6.8839×10^{-5}	-1.7357×10^{-4}	-5.8137×10^{-5}	-5.1647×10^{-5}
Chlorite	-1.0004×10^{-3}	5.3232×10^{-4}	5.6600×10^{-3}	-1.0429×10^{-4}	7.3996×10^{-4}	4.2563×10^{-5}	7.3197×10^{-4}
Quartz	-1.2167×10^{-4}	-2.8004×10^{-6}	9.6515×10^{-7}	7.0201×10^{-3}	4.0357×10^{-5}	-1.3957×10^{-4}	-2.5426×10^{-5}
Feldspar	-2.9205×10^{-5}	-1.8846×10^{-4}	-2.4957×10^{-6}	-7.7438×10^{-6}	2.1365×10^{-3}	8.6977×10^{-5}	-1.4595×10^{-5}
Calcite	5.6658×10^{-5}	3.3377×10^{-6}	1.1196×10^{-6}	1.2928×10^{-7}	1.2185×10^{-5}	1.2825×10^{-3}	-7.4355×10^{-7}
Pyrite	3.1365×10^{-3}	-2.5502×10^{-5}	-2.8685×10^{-3}	9.1995×10^{-4}	3.3232×10^{-3}	3.8773×10^{-4}	1.2022×10^{-2}

Table 3. Measured weight percentages of minerals in standard mixtures and their calculated abundances, using average peak areas from X-ray diffraction and normalization factors determined with matrix singular value decomposition.

Mixture number		Standard mineral in mixture						
		Smectite	Mica	Chlorite	Quartz	Feldspar	Calcite	Pyrite
1	Measured	0.0	54.7	14.8	10.0	12.9	5.0	2.6
	Calculated	0.0	53.9	15.2	9.2	13.5	5.2	3.0
2	Measured	2.4	19.9	2.6	30.2	44.9	0.0	0.0
	Calculated	1.2	18.2	4.0	31.0	45.6	0.0	0.0
3	Measured	10.4	24.9	0.0	24.9	22.3	2.6	14.9
	Calculated	12.0	25.1	0.0	25.3	20.0	2.3	15.3
4	Measured	8.2	9.9	23.2	19.7	39.0	0.0	0.0
	Calculated	13.1	11.3	21.3	19.6	34.7	0.0	0.0
5	Measured	14.7	15.4	10.0	14.9	5.1	35.0	5.0
	Calculated	15.7	16.6	10.2	14.7	5.7	33.8	3.3
6	Measured	3.1	2.0	4.0	84.3	0.0	6.6	0.0
	Calculated	2.7	2.3	4.2	83.4	0.6	6.5	0.2
7	Measured	2.1	4.1	1.2	49.7	32.9	5.9	4.1
	Calculated	1.1	3.4	1.1	48.8	34.1	7.1	4.4
8	Measured	45.3	2.0	19.7	6.9	10.1	14.9	1.0
	Calculated	41.5	2.3	20.7	6.7	12.1	15.4	1.3
9	Measured	20.1	0.0	12.6	5.1	2.7	59.5	0.0
	Calculated	21.2	0.0	11.7	5.6	2.6	58.4	0.4
10	Measured	5.0	2.5	3.1	2.7	17.0	69.7	0.0
	Calculated	4.5	3.9	3.1	2.3	15.6	70.2	0.3
11	Measured	0.0	0.0	25.0	0.0	35.0	20.1	19.9
	Calculated	0.0	0.0	25.0	0.7	35.5	19.4	19.2

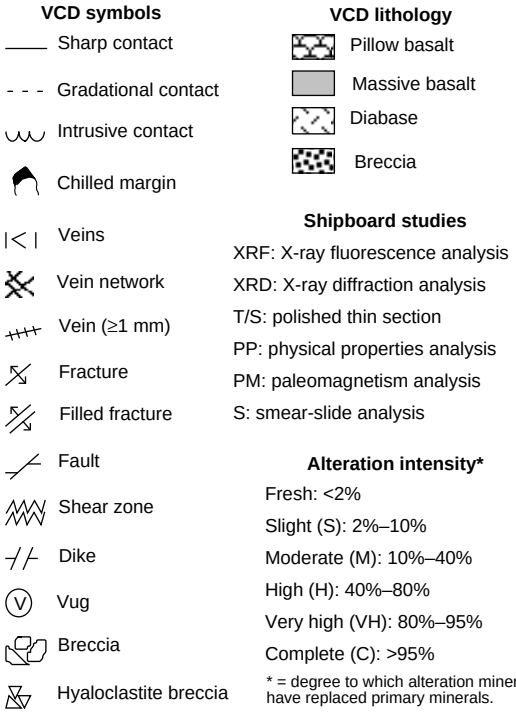

Figure 3. Symbols and terms used on the igneous visual core description forms.

accuracy and to correct for any drift. Table 7 show results obtained by repetitive measurements of basalt standard AII-92-29-1.

CHNS Analyses

In addition to loss on ignition (LOI), total carbon (as CO_2) and structural water (H_2O^+) were determined on rock samples using a Carlo Era NA 1500 CHNS analyzer. Analytical procedures are identical to those used during Legs 140, 147, 148, and 153 (e.g., see Shipboard Scientific Party, 1992b, 1993b, 1995a). The precision and accuracy of this technique were checked against one international reference standard and two shipboard standards (Table 8).

Table 4. Definition of textural terms used to classify all igneous rocks encountered during Leg 168.

Phenocryst abundance
- Aphanitic rocks:
  - Aphyric: <1%
  - Sparsely phyric: 1%–2%
  - Moderately phyric: 2%–10%
  - Highly phyric: >10%

Degree of crystallinity
- Holohyaline: 100% glass
- Hypohyaline: ≥50% glass
- Hypocrystalline: ≥50% crystals
- Holocrystalline: 100% crystals

Grain Size
- Aphanitic rocks:
  - Cryptocrystalline: very fine crystals visible, but not identifiable with a petrographic microscope
  - Microcrystalline: small crystals (≤0.01 mm) identifiable with a petrographic microscope
  - Microlitic: partially crystalline rock containing small euhedral crystals, identifiable with a petrographic microscope
- Phaneritic rocks*:
  - Fine grained: ≤1 mm
  - Medium grained: 1–5 mm

Note: * = average grain size

X-Ray Diffraction Analyses

A variety of alteration minerals were sampled from vein infills within different lithologic units by the shipboard scientists for analysis by XRD. Details of the shipboard procedure and analytical facilities can be found in the "Explanatory Notes" chapter of the Leg 149 *Initial Reports* volume (Shipboard Scientific Party, 1994a).

BIOSTRATIGRAPHY

Biostratigraphy/Paleoenvironments

Only one microfossil group, nannofossils, was examined for biostratigraphic purposes during Leg 168. Because basement ages in the Juan de Fuca region are well known from previous geomagnetic studies (Currie et al., 1982; Johnson and Holmes, 1989; Davis and Currie, 1993), the goal of nannofossil analysis was to provide a high-resolution biostratigraphy of sediments overlying igneous basement

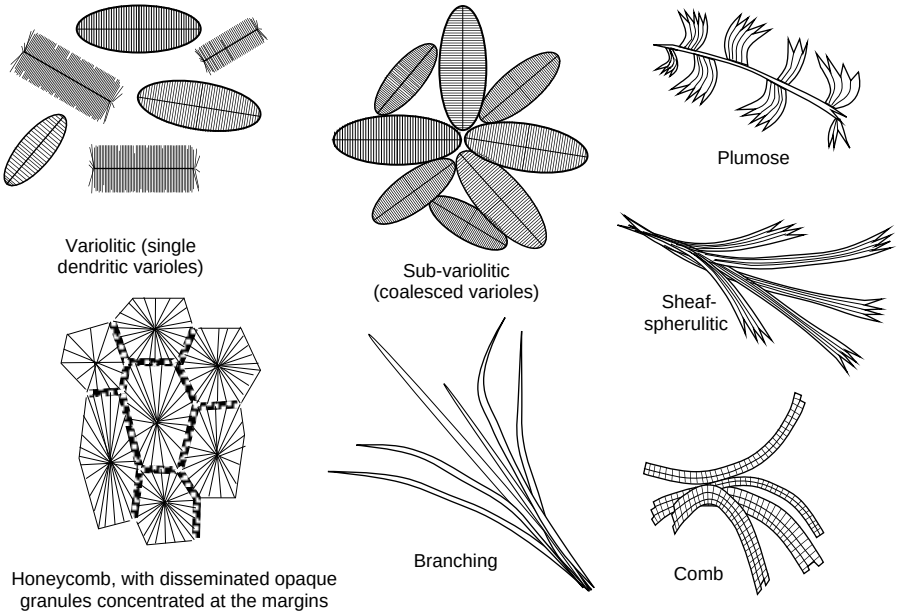

Figure 4. Schematic sketches of different quench textures commonly found within hypocrystalline to hyaline rocks during Leg 168.

Table 5. X-ray fluorescence operating conditions, analytical error estimates, and detection limits.

Oxide (wt%)	Line	Crystal	Detector	Collimator	Peak angle (°2θ)	Background offset (°2θ)	Count time (s)		Analytical error (relt. %)	Detection limit
							Peak	Background		
SiO_2	K-alpha	PET	FPC	Medium	109.21		40		0.30	0.03
TiO_2	K-alpha	LIF200	FPC	Fine	86.14		40		0.37	0.01
Al_2O_3	K-alpha	PET	FPC	Medium	145.12		100		0.40	0.01
Fe_2O_3	K-alpha	LIF200	FPC	Fine	57.52		40		0.20	0.01
MnO	K-alpha	LIF200	FPC	Fine	62.97		100		0.10	0.005
MgO	K-alpha	TLAP	FPC	Medium	45.17	±0.80	150	150	0.60	0.01
CaO	K-alpha	LIF200	FPC	Medium	113.09		40		0.30	0.005
Na_2O	K-alpha	TLAP	FPC	Medium	54.10	−1.20	150	150	3.80	0.03
K_2O	K-alpha	LIF200	FPC	Medium	136.69		100		0.40	0.01
P_2O_5	K-alpha	GE111	FPC	Medium	141.04		100		0.40	0.01

Notes: All major elements are measured using a rhodium X-ray tube operated at 30 kV and 80 mA. relt. % = relative percent. FPC = flow proportional counter (P10 gas).

Table 6. Major element XRF analyses of rock and mineral reference standards following Leg 168 calibration.

Standard	Rock type	SiO_2 (wt%)	TiO_2 (wt%)	Al_2O_3 (wt%)	Fe_2O_3 (wt%)	MnO (wt%)	MgO (wt%)	CaO (wt%)	Na_2O (wt%)	K_2O (wt%)	P_2O_5 (wt%)	Total (wt%)
AII-92-29-1	MORB	50.02	1.77	15.34	10.90	0.18	7.41	11.01	3.06	0.18	0.17	100.02
BAS-140	Diabase (504B)	51.65	0.99	14.64	11.49	0.18	8.41	12.78	1.94	0.01	0.07	102.16
BE-N (BR)	Alkali Basalt	40.16	2.71	10.09	13.21	0.20	13.64	14.27	3.26	1.43	1.10	100.08
BIR-1	Basalt	48.11	0.96	15.32	11.37	0.17	9.61	13.19	1.82	0.04	0.02	100.61
DR-N	Diorite	54.98	1.10	18.04	9.98	0.22	4.55	7.21	2.97	1.81	0.23	101.11
JA-1	Andesite	64.74	0.87	15.37	7.07	0.16	1.64	5.83	3.93	0.80	0.16	100.57
JA-2	Andesite	57.76	0.71	16.19	6.40	0.12	7.71	6.44	3.27	1.91	0.16	100.67
JA-3	Andesite	62.31	0.70	15.73	6.71	0.11	3.89	6.39	3.21	1.45	0.11	100.61
JB-1a	Basalt	53.40	1.32	14.60	9.14	0.15	8.06	9.43	2.80	1.47	0.25	100.63
JB-2	Basalt	51.66	1.16	14.67	14.25	0.21	4.50	9.57	2.00	0.41	0.09	98.51
JB-3	Basalt	50.30	1.45	17.33	11.94	0.19	5.20	9.70	2.69	0.77	0.28	99.85
K1919	Basalt	49.56	2.82	13.54	12.36	0.17	6.82	11.31	2.29	0.55	0.27	99.70
MRG-1	Gabbro	39.17	3.80	8.61	18.11	0.18	13.56	14.73	0.75	0.19	0.06	99.16
NBS-688	Basalt	47.20	1.17	16.87	10.26	0.17	8.43	12.08	2.12	0.20	0.14	98.63

Notes: Most standards were prepared and analyzed in either triplicate or duplicate.

Table 7. Major element analyses of basalt standard AII-92-29-1 obtained during Leg 168.

AII-92-29-1	SiO_2 (wt%)	TiO_2 (wt%)	Al_2O_3 (wt%)	Fe_2O_3 (wt%)	MnO (wt%)	MgO (wt%)	CaO (wt%)	Na_2O (wt%)	K_2O (wt%)	P_2O_5 (wt%)	Total (wt%)
Preferred values	50.02	1.75	15.49	10.85	0.18	7.41	11.16	3.07	0.17	0.16	100.26
Leg 168 average*	50.54	1.76	15.44	10.99	0.17	7.49	11.10	3.13	0.17	0.17	100.95
Leg 168 1σ	0.50	0.02	0.41	0.10	0.02	0.10	0.11	0.05	0.00	0.00	1.02

Note: * = average of 13 analyses run simultaneously with the samples over the length of the cruise.

Table 8. Calculated detection limits and precision estimates for CO_2, H_2O^+, and S analyses performed on Leg 168 basalts.

	Estuarine sediment (NBS-1646)		Diabase (BAS 140)			Basalt (AII-92-29-1)		
Standard reference	Leg 148	Leg 168	Leg 148	Sparks and Zuleger (1995)*	Leg 168	Leg 140	Staudigel (1979)†	Leg 168
H_2O (wt%)	6.12	5.07	1.41	1.12	1.08	0.91	1.05	0.78
1σ	0.37	0.27	0.02	0.14	0.21	0.08	0.07	0.1
CO_2 (wt%)	6.37	6.31	0.07	0.05	0.09	0.07	—	0.06
1σ	0.28	0.51	0.01	0.03	0.06	0.01	—	0.05
S (wt%)	—	—	—	0.09	0.03	—	—	0.05
1σ	—	—	—	0.0048	0.02	—	—	0.005

Notes: * = average values collated from three different laboratories, as reported in Sparks and Zuleger (1995). † = average values computed from six of nine analyses reported by different international laboratories in Staudigel (1979). Three analyses that deviated more than 1σ from the entire data set were discarded. wt% = weight percent, and — = not analyzed.

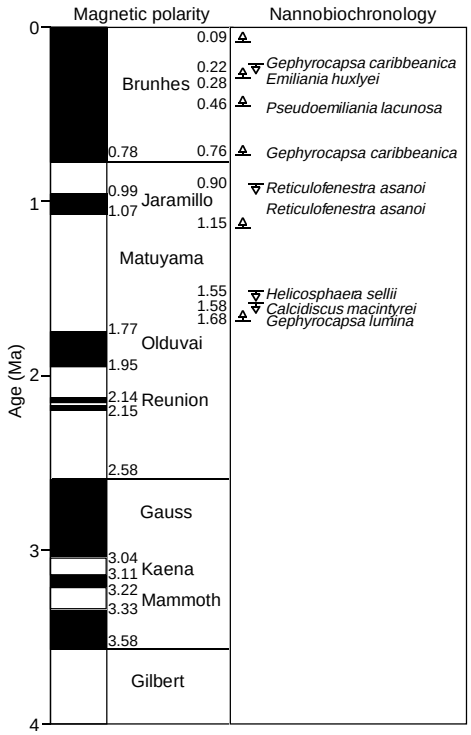

Figure 5. Magnetic polarity and nannofossil time scale used during Leg 168 age-profile studies.

ranging from 0.78 to 3.55 Ma in age. To obtain more detailed records, nannofossil age assignments during Leg 168 were made on a number of samples within each core (one or two samples per section) instead of only on samples from core catchers.

Late Cenozoic assemblages in the Juan de Fuca region are characterized by low species diversity and by abundant cold-water species, such as *Coccolithus pelagicus*, *Gephyrocapsa muellerae*, and *Gephyrocapsa caribbeanica*, and abundant cosmopolitan species (e.g., *Emiliania huxleyi*). Tropical and subtropical species (e.g., Pliocene marker species of the genus *Discoaster*) are absent, and only a few temperate species (e.g., *Helicosphaera carteri*) are sporadic in analyzed samples. As a result, only a few Quaternary nannofossil datums are useful for Leg 168.

In the Quaternary, a few *Gephyrocapsa* species are used as biostratigraphic markers. The method for separating and identifying *Gephyrocapsa* species follows Su (1996).

The nannofossil datum ages used for Leg 168 are based on Su (1996, Northeast Atlantic) and on Shipboard Scientific Party (in press; Leg 167, California Margin). These datums are calibrated to the Cande and Kent (1995) geomagnetic polarity time scale (Fig. 5).

Method

Smear slides were prepared using standard techniques, and nannofossils were examined by means of standard light microscope techniques at magnifications ranging from 1000× to 2000×.

Nannofossil abundances, preservations, and age or zone were recorded for each sample using the computer program FossiList. Degrees of fossil abundance and preservation are given in Table 9.

PALEOMAGNETISM

Leg 168 paleomagnetism studies concentrated on sediment core magnetostratigraphy. The primary objectives of the magnetostratigraphy studies were to determine a sedimentation rate/age profile at each site, in collaboration with the shipboard biostratigraphy studies of the mixed turbidite and pelagic sequences. At Circulation Obviation Retrofit Kit (CORK) sites (1024–1027) where basaltic basement was recovered, an additional objective was to characterize the basic magnetic properties of the basalts (natural remanent magnetization [NRM] directions and intensities, susceptibility, and remanence directions). Results from basement samples are not reported here (see below).

Laboratory Facilities

A new 2G Enterprises (Model 760R) pass-through cryogenic magnetometer was installed during the port call at the start of Leg 168. The new direct current (DC) superconducting quantum interface devices (SQUIDS) in the magnetometer have a response function that provides a spatial resolution of ~7 cm, considerably better than the RF SQUIDS (~20 cm) of the previous cryogenic magnetometer. The new cryogenic magnetometer SQUIDS have a sensitivity of 3–5 × 10^{-8} emu, which permits the measurement of considerably lower intensity samples than previously possible. Declination and inclination data are derived from the moment measurements along the three orthogonal sensors.

However, the accompanying software for driving the new machine created difficulties and much additional work for the paleomagnetist and paleomagnetics technician. After several weeks of testing the software, they decided to program new driver software in Labview; by the second half of the leg a working version was ready to use. However, there was no data reduction software provided with the new machine, which forced the paleomagnetist to reduce the data using Excel spreadsheets. Exact determination of the new cryogenic system response functions could not be achieved during the cruise; therefore, the shipboard data reduction was an approximation. After Leg 168, the exact system response functions were determined, which enabled the shipboard data to be reprocessed. However, because of time constraints on submitting results to the ODP *Initial Reports* volume, only part of the data for sediment magnetostratigraphy

Table 9. Degrees and definitions of fossil preservation and abundance used during Leg 168, after the computer program FossiList.

Degrees	Definition
Preservation	
P	Poor: strong overgrowth and dissolution, most specimens fragmented and hard to identify
P–M	Poor–moderate: moderate to strong overgrowth and dissolution
M	Moderate: moderate overgrowth and dissolution, most taxa readily identified
M–G	Moderate–good: slight to moderate overgrowth and dissolution
G	Good: slight overgrowth or dissolution, all taxa easily identified
VG	Very good: pristine preservation, no overgrowth or dissolution
Dissolution	
1	No dissolution
2	>50% of specimens slightly etched: all taxa easily identified
3	>50% of specimens moderately etched: >50% taxa readily identified
4	>50% of specimens strongly etched and fragmented: low diversity
5	Almost all specimens strongly etched and fragmented: all species rare
6	Maximum dissolution: barren of coccoliths
Overgrowth	
1	No overgrowth
2	>50% of specimens slightly overgrown: all taxa easily identified
3	>50% of specimens moderately overgrown: >50% taxa readily identified
4	>50% of specimens strongly overgrown: low diversity
5	Almost all specimens strongly overgrown: all species rare
6	Maximum overgrowth, limestone or calcareous debris: barren of identifiable coccoliths
Group abundance and species abundance	
B	Barren: 0 (note this degree is used only for the group abundance)
P	Present: <0.1%
T	Trace: 0.1%–1.0%
R	Rare: 1%–5%
F	Few: 5%–10%
C	Common: 0%–30%
A	Abundant: 30%–60%
D	Dominant: >60%

was completed. Results from the remaining sediments, and from basement samples, will be reported elsewhere.

An in-line alternating field (AF) demagnetizer (Model 2G600) was used with the pass-through magnetometer. The AF coils are capable of producing a maximum alternating field of 80 mT.

Low-Field Susceptibility

Whole-core magnetic susceptibility (k) was measured at 3-cm intervals using the Bartington Instrument susceptibility meter (Model MS1) as part of the multisensor track (MST) measurements. MST data were measured before some of the whole-round samples were taken. These data are directly comparable with the pass-through magnetometer data; however, there are cores for which susceptibility data were collected that were not run in the cryogenic magnetometer because of high levels of drilling-related disturbance. Susceptibility data have been archived in volume normalized $\times 10^{-5}$ SI units. Bulk susceptibility was measured for all discrete samples using either the Kappabridge KLY-2 susceptibility bridge or the Bartington magnetic susceptibility meter (Model MS2).

Paleomagnetic Measurements

Continuous core paleomagnetic measurements were performed on the archive half of cores for ~90% of the advanced hydraulic piston corer (APC) sediment cores, ~75% of the extended core barrel (XCB) sediment cores (depending on degree of drilling disturbance), and all orientable pieces (those with a length greater than the width of the core liner, or ~5 cm) of the rotary core barrel (RCB) basement cores. The NRM and remanence directions were measured after 20- or 25-mT demagnetization for the archive half of sediment cores. The basalt and diabase cores recovered during Leg 168 have exceptionally strong NRM intensities (20–45 A/m), which vastly exceed the limits of the DC SQUIDS. To overcome this, selected oriented pieces were taken from the archive half and measured individually in the magnetometer. The NRM and remanence directions were measured after 5-, 10-, 15-, and 20-mT demagnetization for the individual basement archive core pieces; these data will be reported at a later date. All continuous core measurements were made at 10-cm intervals. All magnetic data are reported relative to the standard ODP paleomagnetic coordinate system (Shipboard Scientific Party, 1995a).

Many of the cores recovered in the sediment sections exhibited drilling-related disturbance. APC cores that exhibited a large amount (~10%) of flow-in, as evident from highly convex-upward bedding planes throughout the cores, were not measured because directions obtained were likely to be unreliable. A large number (~50%) of the XCB cores showed evidence of drilling-related disturbance of the sediments in the form of liquefied coarse sand units and biscuiting of semilithified sediments. Data from liquefied sand units were removed from the data set after measurements were taken. Core sections with <5-cm-thick biscuits surrounded by an equal to greater volume of drilling-derived muds were not measured. Only XCB cores with >50% sediment biscuits (as >10-cm-thick biscuits) were measured.

Discrete 7-cm^3 sediment samples and 10-cm^3 minicore basement samples were stepwise demagnetized to determine characteristic remanence directions for specific sections of the cores. NRM directions and intensities were measured both with the Molspin magnetometer, using the PMagic program (version 1.2), and with the cryogenic pass-through magnetometer, using the discrete sample option menu in the 2G long core program (version 1.0). NRM measurements were made on both magnetometers to provide a calibration between the two instruments. The samples were stepwise demagnetized using either the Schonstedt AF demagnetizer (Model GSD-1) or the AF coils, which are in line with the cryogenic pass-through magnetometer. The Schonstedt demagnetizer demagnetized samples along the positive axis directions (+x, +y, and +z) and the negative axis directions (–x, –y, –z) at alternating demagnetization steps to identify spurious anhysteretic remanence.

Magnetostratigraphy

A combined nannofossil and magnetic polarity time scale (Fig. 5) was used by the shipboard paleontologists and paleomagnetist based upon the Pliocene–Pleistocene polarity boundaries of Cande and Kent (1995). Magnetic reversals were identified primarily using the 20- to 25-mT continuous core demagnetization inclination. The declination data were used in the analysis of complex polarity zones

where the inclination data alone were ambiguous. These intervals may represent a number of geologic and/or magnetic scenarios, including excursions of the magnetic field, an input of terrigenous material during turbidite sedimentation, and drilling-related disturbance of the magnetic signal.

PHYSICAL PROPERTIES

Introduction

The primary objectives of Leg 168 included characterizing the physical effects of, and controls on, ridge flank hydrothermal circulation. To fulfill this objective, the physical properties program was designed to (1) look for physical evidence of alteration in the sediments caused by past or present fluid flow; (2) estimate compaction patterns as they vary laterally and with depth, which might correspond to the evolution of the flank hydrothermal system; (3) examine the relationship between velocity, porosity, and depth to aid in the interpretation of seismic data; and (4) determine the thermal conductivity structure of the sediments to calculate heat flow from downhole temperature data and estimate temperatures at depth from seafloor heat-flow data.

Sediments recovered comprise hemipelagic muds and interbedded turbidite sequences. To more clearly identify trends in the data, physical properties results for the sediments are separated into two groups: mud and sand, according to the visual core descriptions. Sand includes the lithologic facies sand/silt/clay, sand/sandstone, silty sand/sandy silt, and sandy clay/clayey sand, whereas mud includes all material excluded from the sand group. The mud category contains only fine material, whereas the sand category contains a mixture of coarse and fine sand, as it was difficult to identify the tops of common, graded turbidite layers. This division probably does not separate these units according to mode of deposition or sediment source area, but it is an important one for interpreting the data because grain size exerts a major control on physical properties.

Core Handling

Soon after the cores were cut into 1.5-m sections and the 15-cm-long interstitial water whole-round samples were taken, the sections were passed through the MST, which makes several high-resolution measurements. This was usually done before the sections thermally equilibrated so that MST information was available as quickly as possible and could be used to aid in the selection of additional whole-round samples and positions for thermal conductivity measurements before cores were split. Following the MST measurements, the cores were set aside to equilibrate to lab temperature (about 2 hr). Thermal conductivity measurements in soft sediment were made before equilibrated cores were split. Index properties, *P*-wave velocity, shear strength, and electrical resistivity measurements on all lithologies, as well as thermal conductivity measurements on lithified sediment and basalt, were made on split cores.

Because of core handling procedures, basalt cores usually dried before they were available for physical properties sampling. Samples for measurements were resaturated in seawater for at least 12 hr under normal laboratory conditions before being measured.

Multisensor Track

The MST provided measurements of bulk density, compressional wave velocity, magnetic susceptibility, and natural gamma radiation in unsplit cores using the gamma-ray attenuation porosity evaluator (GRAPE; 5-cm spacing, 4-s period), P-wave logger (PWL; 5-cm spacing, 5- s period), magnetic susceptibility meter (MSM; 3-cm spacing, 1-s period), and natural gamma-ray (NGR) detector (15-cm spacing, 5-s period), respectively. A detailed description of the MST is given in the "Physical Properties" section of the "Explanatory Notes" chapter of the Leg 159 *Initial Reports* volume (Shipboard Scientific Party, 1996c).

For the RCB cores, the core liner was split and the pieces were separated with plastic spacers in the working half of the core liner. MST measurements were run with the archive half of the core liner removed. The pieces were then split, and the split cores made available for Digital Sonic Velocimeter (DSV) and thermal conductivity tests. The MSM showed unrealistic low values at the ends of each section. Such low values (e.g., bulk density below 1 g/cm^3 and thermal conductivity below 0.6 W/[m·K]) were erased from the data set. We also filtered out PWL measurements with signal strengths (digitized peak voltage of the largest value from the received signal after amplification) below 100.

Locations of Subsequent Measurements

The majority of the sedimentary units comprise sand and mud sequences with variable physical properties. To ensure that measurements were clustered within consistent lithologic units and did not cross lithologic boundaries, subsequent sample and measurement locations were chosen using the magnetic susceptibility data. Sand layers were identified as having relatively high magnetic susceptibility values compared to mud.

Thermal Conductivity

Methods for thermal conductivity measurements on ODP cruises are described in detail in the "Explanatory Notes" chapter of the Leg 139 *Initial Reports* volume (Shipboard Scientific Party, 1992a). Once the core sections equilibrated at room temperature, we measured thermal conductivity of the whole sections with the needle probe methods using the ThermCon 85 instrument.

For lithified sediments and basalt a new device, the TK04, was used to measure the thermal conductivity with a half-space line source. The TK04 is based on the same principle of a continuously heated line source as ThermCon 85, but the evaluation method is improved and automated. The standard approach is to plot the source temperature against the logarithm of heating time; thermal conductivity is calculated from the slope of this curve in an interval where the increase is apparently linear and as free as possible from non-ideal behavior at early and late times. The position and length of this interval are related primarily to the time constant of the probe in sediment, the contact resistance between the probe and rock early in the measurement, and the size and thermal diffusivity of the sample late in the measurement. Instead of calculating the thermal conductivity in a fixed time interval, the TK04 algorithm performs linear regressions in a large number of time intervals and determines the best fit. The range and the minimum and maximum lengths of possible intervals are specified by the operator. Another option is to evaluate the data by fitting the source temperature for these time intervals to the analytical solution of a constantly heated line source (Special Approximation Method [SAM]). This method provides a criterion with physical relevance to determine the optimal time interval (for more information, see the TK04 manual).

The TK04 includes full-space needle probes and half-space line sources. The probes were not calibrated aboard the ship because they were tested by the manufacturer before delivery; the accuracy is cited to be ±5%. Measurements with the needle probe (full-space geometry) of available standards were not possible because the TK04 needle diameter is slightly larger than the ThermCon 85 needle diameter, and drill bits with the necessary dimensions were not available on board. The TK04 half-space line source reproduced the thermal conductivity of ODP standards well, however, as follows: Macor: ODP value 1.61 ± 0.08 W/(m·K), TK04 value 1.63 ± 0.05 W/(m·K); basalt: ODP value 2.05 ± 0.10 W/(m·K), TK04 value 2.02 ± 0.03 W/(m·K).

Two different procedures for routine measurements were chosen for the full- and half-space measurements. The needle probes are gen-

erally used in soft sediments, which have high water contents. The preferable evaluation method, SAM, is too sensitive to small disturbances (e.g., convecting pore water during the heating of the probe). Thus, the more robust linear fit method was used for full-space probe measurements. The appropriate parameters are a heating power of 1 W/m and evaluation intervals between 40 and 300 s with a minimum length of 240 s. Generally, three repeat measurements were performed and the results averaged.

The half-space line source can be used on split cores for both soft and hard sediment; it fits into the split liner. Here, the SAM is more appropriate. The half-space parameters are a heating power of 3 W/m and evaluation intervals between 25 and 80 s with a minimum length of 25 s. Generally, three repeat measurements were performed and the results averaged. Semilithified sediment was measured in the split liner, and the surface was wetted with water for better contact. Harder pieces and basalt samples were removed from the liner, and measurements were performed by immersing the sample and the half-space line source in water.

Results from the TK04 are included in the data sets; however, because the system was used for the first time, most routine full-space needle probe measurements were made with the ThermCon 85. All half-space probe measurements were made with the TK04.

Digital Sonic Velocimeter and Shear Strength

The DSVs were used to obtain *P*-wave velocities in three directions. The velocities parallel and perpendicular to the core axis (parallel to the cut plane), as well as perpendicular to the core axis and perpendicular to the cut plane, were determined with DSVs 1, 2, and 3, respectively. Unlike the *P*-wave measurements of the MST, the first arrival was chosen manually. In more lithified cores, when the biscuits were hard enough to be removed from the core liner and clamped between transducers, we measured the velocity along the core axis as well as parallel to the beds in the Hamilton Frame Velocimeter (DSV 3).

Undrained shear strength was measured by a modified Wykeham Farrance Laboratory Vane Apparatus (Boyce, 1977). A computer controlled and monitored the torque and the strain rates until failure. The procedures for measuring velocity and shear strength are described in detail in the "Physical Properties" section of the "Explanatory Notes" chapter of the Leg 159 *Initial Reports* volume (Shipboard Scientific Party, 1996c).

Electrical Resistance and Formation Factor

Electrical resistance measurements were used to determine a formation factor. The electrodes were spaced in a Wenner spread configuration, with 12-mm-long, 1.5-mm-diameter electrodes spaced 15 mm apart. Resistance was measured using a Wayne Kerr Precision Component Analyzer 6425. The formation factor is calculated as the ratio of resistance in the sediment along the core axis to resistance of seawater at the same temperature held in a 30-cm-long section of split core liner.

Two or three measurements were usually taken per core section. Where the lithification of sediments prevented the probe insertion without the sediments breaking, holes of the same diameter and spacing as the electrodes were drilled into the sediment, and the probe, wet with seawater, was carefully inserted. For each measurement in the sediment, there was a corresponding measurement of seawater resistance.

Index Properties

Bulk density, grain density, water content, and porosity were determined from 10-cm^3 samples taken from split cores. The wet mass of the sample was measured and then the sample was placed in a 105°C oven and allowed to dry for more than 24 hr. The dry mass was then measured, and the dry volume was determined using a Quantachrome Penta-Pycnometer. Index properties were then calculated using "Method C," as described in detail in the "Physical Properties" section of the "Explanatory Notes" chapter of the Leg 158 *Initial Reports* volume (Shipboard Scientific Party, 1996a).

SAMPLING AND CHEMICAL ANALYSES OF INTERSTITIAL WATER

Shipboard interstitial water analyses were performed routinely on 10- to 25-cm-long whole-round sections that were cut immediately after the core arrived on deck. Interstitial waters were retrieved using a titanium squeezer (Manheim and Sayles, 1974) at as much as 275 MPa (40,000 psi) pressure, applied with a hydraulic press, and were filtered through a 0.45-µm polycarbonate filter.

Four samples from Site 1026 were analyzed after the MST data had been collected, a few hours after core collection and after equilibration to room temperature. Analyses showed a decrease in chlorinity and significant differences in alkalinity and in alkaline earth concentrations when compared to samples from the same cores squeezed soon after recovery. Therefore, MST data could not be used to guide core sampling for interstitial water.

Interstitial water samples were analyzed routinely for salinity as total dissolved solids with a Goldberg optical refractometer. Alkalinity and pH were measured by Gran titration with a Metrohm autotitrator and a Brinkmann pH electrode standardized with NBS buffers at pHs 4, 7, and 10. Magnesium was determined by complexiметric titration (Gieskes et al., 1991); calcium and chloride, by electrochemical titration. Mg and Ca were also measured by ion chromatography using a Dionex DX-100. Results were indistinguishable except at low Mg concentration, and for this reason Mg was additionally analyzed in such samples using a Varian SpectrAA-20 atomic absorption unit with an air-acetylene flame. Silica, phosphate, ammonia, and boron concentrations were determined by spectrophotometric methods using a Milton Roy Spectronic 301 spectrophotometer as described by Gieskes et al. (1991). Potassium and sulfate were obtained by ion chromatography, which proved unreliable for Cl. Sodium was calculated from the electoneutrality condition.

ORGANIC GEOCHEMISTRY

The shipboard organic geochemical investigations for Leg 168 included (1) real-time monitoring of hydrocarbon gases as required for ODP safety considerations; (2) measurement of inorganic carbon to determine the amount of carbonate in the sediments; (3) elemental analyses of total carbon, sulfur, nitrogen, and hydrogen; and (4) initial characterization of the amount, origin, and maturity of organic matter. These procedures were conducted to provide a basis for the site summaries and background for more detailed shore-based research. Methods and instruments are described in more detail by Emeis and Kvenvolden (1986) and Kvenvolden and McDonald (1986).

As required for safety considerations, the concentrations of the light hydrocarbons methane (C_1), ethane (C_2), propane (C_3), ethylene (C_2=), and propylene (C_3=) were monitored in one headspace sample from each core. Details of headspace sampling and analysis are given in the "Explanatory Notes" chapter of the Leg 167 *Initial Reports* volume (Shipboard Scientific Party, in press).

Total inorganic carbon was determined using a Coulometrics 5011 carbon dioxide coulometer equipped with a System 140 carbonate carbon analyzer. Sediments were analyzed at a frequency of one sample per section. Approximately 10 mg of freeze-dried and ground sediment was analyzed as described in the "Explanatory Notes" chapter of the Leg 160 *Initial Reports* volume (Shipboard Scientific Party, 1996d). The weight percentage of carbonate was calculated

from the inorganic carbon (IC) content, simply assuming that all carbonate occurs as calcium carbonate:

$$CaCO_3 = IC \times 8.33.$$

Total carbon, hydrogen, nitrogen, and sulfur of sediment samples were determined using a Carlo Erba NA 1500 NCHS analyzer. The elemental analyses were performed on one sample per core and followed the method described in the "Explanatory Notes" chapter of the Leg 155 *Initial Reports* volume (Shipboard Scientific Party, 1995b). Total organic carbon (TOC) was calculated as the difference between total carbon (TC) from the NCHS analyzer and total IC from the coulometer:

$$TOC = TC - IC.$$

The type and maturity of organic matter were evaluated by pyrolysis using a Delsi Nermag Rock-Eval II system (Espitalié et al., 1986). Analyses were performed on sediment samples prepared for carbonate and elemental analysis containing at least 0.5 wt% TOC because interpretation of Rock-Eval pyrolysis data is considered unreliable for samples containing less than 0.5 wt% TOC (Peters, 1986). For details of the method and interpretation of Rock-Eval pyrolysis data, see Tissot and Welte (1984) and the "Explanatory Notes" chapter of the Leg 146 *Initial Reports* volume (Shipboard Scientific Party, 1994b)

DOWNHOLE TOOLS

We used a variety of tools for subseafloor experiments during Leg 168. The techniques employed were very similar to those used during Legs 139 and 164, when many of these tools were used to great advantage. The tools and methods used in deployment and data analysis are described in the following publications:

1. Adara temperature tool downhole measurements: Shipboard Scientific Party (1992a).
2. Water-sampling temperature probe: Shipboard Scientific Party (1992a).
3. Davis/Villinger Temperature Probe: Davis et al. (1997).
4. Packer experiments: Shipboard Scientific Party (1992a); Becker et al. (1994).
5. Circulation Obviation Retrofit Kit: Davis et al. (1992) and as discussed below.
6. Logging measurements: Shipboard Scientific Party (1996b), with exceptions noted below.

CORK OsmoSampler

A new tool deployed in CORKed holes during Leg 168 and previously at Site 949 in the Barbados accretionary prism during Leg 156 (Shipboard Scientific Party, 1995c) is the OsmoSampler. OsmoSamplers, osmotically pumped fluid samplers, have been designed to collect continuous uncontaminated seawater from basaltic basement for a period of 5 yr. Technology for the osmotic pump sampler was developed by Hans Jannasch (Monterey Bay Aquarium Research Institute) to provide a long-term electronic-free sampler without moving parts. OsmoSamplers are driven by molecular diffusion of water through a rigid semipermeable membrane that separates a saturated salt solution from distilled water. The resulting osmotic pressure is used to pull water through one membrane at a rate of about 4 µL/hr at 20°C. The precise rate of flow is determined by the number of membranes (surface area) and temperature, as the rate of flow increases with increasing temperature. Osmotic pumps draw from a distilled water reservoir, which in turn, is connected to a small-bore Teflon tube (1.0-mm ID) that is open at the sampling port. The length of this tubing is selected on the basis of the expected duration of the deployment and rate of flow. Although diffusion tends to integrate samples with different compositions, the characteristic distance for molecular diffusion is less than 2 m for the 5-yr duration of the Leg 168 CORK experiments (Jannasch et al., 1996).

OsmoSamplers were designed, fabricated, and deployed in each of the holes in which a CORK was installed during ODP Leg 168. These samplers were designed to fit through the CORK annulus (7.62-cm OD) and to fit over the deepest portion of the thermistor string with a 2.54-cm ID polycarbonate tube. OsmoSamplers were tied to thermistor strings near the deepest thermistor so that temperature and thus rate of pumping would be known for the life of the experiment.

The goal was to design a pump to draw 50 µL/hr of seawater. This rate of pumping is achieved with eight membranes at about 40°C or three membranes at 70°C, approximately equivalent to the basement temperatures at ODP Site 1025 and the Rough Basement sites, respectively. Because of the cooler temperatures and the physical constraints that limit the number of membranes to eight, the OsmoSampler at Site 1024 (23°C) will draw only half of the desired rate. A rate of 50 µL/hr results in 8.4 mL of sample per week for a total of 2.2 L in 5 yr. This volume requires about 2.1 km of 1.0-mm ID Teflon tubing. Only 1.2 km of tubing was deployed at Site 1024.

We expect to retrieve these OsmoSamplers about 4 yr after deployment when the CORK temperature/pressure experiments have been completed. Weekly samples will be analyzed for the major and some minor ions in seawater. The stable isotopic compositions of Sr, H, O, C, B, and Cl also will be measured.

Downhole Logging

Three tool strings were run during Leg 168: triple combination, Formation MicroScanner, and geochemical. The triple combination string comprised phasor induction, spectral gamma-ray, porosity, and lithodensity tools. The spectral gamma-ray and porosity tools run with the triple combination string were new models run for the first time during Leg 166. The Formation MicroScanner string included Formation MicroScanner, array sonic, and spectral gamma tools. The geochemical string comprised geochemical spectroscopy, aluminum activation, compensated neutron (used as a source for the aluminum activation measurements), and spectral gamma tools.

Log processing procedures generally followed those described by the Shipboard Scientific Party (1996b). The triple combination run in Hole 1032A provided the depth reference for subsequent logging runs. Oxide/carbonate normalization factors for the processing of geochemical data are included in Table 10.

REFERENCES

Becker, K., Morin, R.H., and Davis, E.E., 1994. Permeabilities in the Middle Valley hydrothermal system measured with packer and flowmeter experiments. *In* Mottl, M.J., Davis, E.E., Fisher, A.T., and Slack, J.F. (Eds.), *Proc. ODP, Sci. Results*, 139: College Station, TX (Ocean Drilling Program), 613–626.

Boyce, R.E., 1977. Deep Sea Drilling Project procedures for shear strength measurement of clayey sediment using modified Wykeham Farrance laboratory vane apparatus. *In* Barker, P.F., Dalziel, I.W.D., et al., *Init. Repts. DSDP*, 36: Washington (U.S. Govt. Printing Office), 1059–1068.

Cande, S.C., and Kent, D.V., 1995. Revised calibration of the geomagnetic polarity timescale for the Late Cretaceous and Cenozoic. *J. Geophys. Res.*, 100:6093–6095.

Currie, R.G., Seemann, D.S., and Riddihough, R.P., 1982. Total magnetic field anomaly, offshore British Columbia. *Open File Rep.—Geol. Surv. Can.*, 828.

Davis, E.E., Becker, K., Pettigrew, T., Carson, B., and MacDonald, R., 1992. CORK: a hydrologic seal and downhole observatory for deep-ocean boreholes. *In* Davis, E.E., Mottl, M.J., Fisher, A.T., et al., *Proc. ODP, Init. Repts.*, 139: College Station, TX (Ocean Drilling Program), 43–53.

Davis, E.E., and Currie, R.G., 1993. Geophysical observations of the northern Juan de Fuca Ridge system: lessons in sea-floor spreading. *Can. J. Earth Sci.,* 30:278–300.

Davis, E.E., Villinger, H., MacDonald, R.D., Meldrum, R.D., and Grigel, J., in press. A rapid-response probe for bottom-hole temperature measurements in deep-ocean boreholes. *Mar. Geophys. Res.*

Emeis, K.-C., and Kvenvolden, K.A., 1986. Shipboard organic geochemistry on *JOIDES Resolution. ODP Tech. Note*, 7.

Espitalié, J., Deroo, G., and Marquis, F., 1986. La pyrolyse Rock-Eval et ses applications, Partie III. *Rev. Inst. Fr. Pet.,* 41:73–89.

Fisher, A.T. and Underwood, M.B., 1995. Calibration of an X-ray diffraction method to determine relative mineral abundances in bulk powders using matrix singular value decomposition: a test from the Barbados accretionary complex. *In* Shipley, T.H., Ogawa, Y., Blum, P., et al., *Proc. ODP, Init. Repts.,* 156: College Station, TX (Ocean Drilling Program), 29–37.

Gieskes, J.M., Gamo, T., and Brumsack, H., 1991. Chemical methods for interstitial water analysis aboard *JOIDES Resolution. ODP Tech. Note,* 15.

Govindaraju, K., 1989. 1989 compilation of working values and sample description for 272 geostandards. *Geostand. Newsl.,* 13 (spec. iss.).

Harvey, P.K., Taylor, D.M., Hendry, R.D., and Bancroft, F., 1973. An accurate method for the analysis of rocks and chemically related materials by X-ray fluorescence spectrometry. *X-Ray Spectrom.,* 2:33–44.

Jannasch, H.W., Wheat, C.G., Kastner, M., and Stakes, D., 1996. Sample resolution in long-term osmotically pumped continous fluid samplers. *Eos,* 77: F725.

Johnson, H.P., and Holmes, M.L., 1989. Evolution in plate tectonics: a study of the Juan de Fuca Ridge. *In* Winterer, E.L., Hussong, D.M., and Decker, R.E. (Eds.), *The Eastern Pacific Ocean and Hawaii.* Geol. Soc. Am., Geol. of North Am. Ser., N:73–91.

Kvenvolden, K.A., and McDonald, T.J., 1986. Organic geochemistry on the *JOIDES Resolution*—an assay. *ODP Tech. Note,* 6.

Manheim, F.T., and Sayles, F.L., 1974. Composition and origin of interstitial waters of marine sediments, based on deep sea drill cores. *In* Goldberg, E.D. (Ed.), *The Sea* (Vol. 5): *Marine Chemistry: The Sedimentary Cycle:* New York (Wiley), 527–568.

Mazzullo, J., and Graham, A.G. (Eds.), 1988. Handbook for Shipboard Sedimentologists. *ODP Tech. Note*, 8.

Mazzullo, J.M., Meyer, A., and Kidd, R.B., 1988. New sediment classification scheme for the Ocean Drilling Program. *In* Mazzullo, J., and Graham, A.G. (Eds.), Handbook for Shipboard Sedimentologists. *ODP Tech. Note,* 8:45–67.

McKenzie, W.S., Donaldson, C.H., and Guilford, C., 1982. *Atlas of Igneous Rocks and Their Textures:* New York (Longman Scientific & Technical; Wiley.)

Peters, K.E., 1986. Guidelines for evaluating petroleum source rock using programmed pyrolysis. *AAPG Bull.,* 70:318–329.

Schneider, R.R., Cramp, A., Damuth, J.E., Hiscott, R.N., Kowsmann, R.O., Lopez, M., Nanayama, F., Normark, W.R., and Shipboard Scientific Party, 1995. Color-reflectance measurements obtained from Leg 155 cores. *In* Flood, R.D., Piper, D.J.W., Klaus, A., et al., *Proc. ODP, Init. Repts.,* 155: College Station, TX (Ocean Drilling Program), 697–700.

Shipboard Scientific Party, 1989. Explanatory notes. *In* Robinson, P.T., Von Herzen, R.P., et al., *Proc. ODP, Init. Repts.,* 118: College Station, TX (Ocean Drilling Program), 3–23.

————, 1992a. Explanatory notes. *In* Davis, E.E., Mottl, M.J., Fisher, A.T., et al., *Proc. ODP, Init. Repts.,* 139: College Station, TX (Ocean Drilling Program), 55–97.

————, 1992b. Explanatory notes. *In* Dick, H.J.B., Erzinger, J., Stokking, L.B., et al., *Proc. ODP, Init. Repts.,* 140: College Station, TX (Ocean Drilling Program), 5–33.

————, 1993a. Explanatory notes. *In* Alt, J.C., Kinoshita, H., Stokking, L.B., et al., *Proc. ODP, Init. Repts.,* 148: College Station, TX (Ocean Drilling Program]), 5–24.

————, 1993b. Explanatory notes. *In* Gillis, K., Mével, C., Allan, J., et al., *Proc. ODP, Init. Repts.,* 147: College Station, TX (Ocean Drilling Program), 15–42.

————, 1994a. Explanatory notes. *In* Sawyer, D.S., Whitmarsh, R.B., Klaus, A., et al., *Proc. ODP, Init. Repts.,* 149: College Station, TX (Ocean Drilling Program), 11–34.

————, 1994b. Explanatory notes. *In* Westbrook, G.K., Carson, B., Musgrave, R.J., et al., *Proc. ODP, Init. Repts.,* 146 (Pt. 1): College Station, TX (Ocean Drilling Program), 15–48.

————, 1995a. Explanatory notes. *In* Cannat, M., Karson, J.A., Miller, D.J., et al., *Proc. ODP, Init. Repts.,* 153: College Station, TX (Ocean Drilling Program), 15–42.

————, 1995b. Explanatory notes. *In* Flood, R.D., Piper, D.J.W., Klaus, A., et al., *Proc. ODP, Init. Repts.,* 155: College Station, TX (Ocean Drilling Program), 62–63.

————, 1995c. Site 949. *In* Shipley, T.H., Ogawa, Y., Blum, P., et al., *Proc. ODP, Init. Repts.,* 156: College Station, TX (Ocean Drilling Program), 193–257.

————, 1996a. Explanatory notes. *In* Humphris, S.E., Herzig, P.M., Miller, D.J., et al., *Proc. ODP, Init. Repts.,* 158: College Station, TX (Ocean Drilling Program), 37–53.

————, 1996b. Explanatory notes. *In* Jansen, E., Raymo, M.E., Blum, P., et al., 1996, *Proc. ODP Init. Repts.,* 162: College Station, TX (Ocean Drilling Program), 21–45.

————, 1996c. Explanatory notes. *In* Mascle, J., Lohmann, G.P., Clift, P.D., et al., 1996. *Proc. ODP, Init. Repts.,* 159: College Station, TX (Ocean Drilling Program).

————, 1996d. Explanatory notes. *In* Emeis, K.-C., Roberston, A.H.F., Richter, C., et al., *Proc. ODP, Init. Repts.,* 160: College Station, TX (Ocean Drilling Program), 43–44.

————, in press. Explanatory notes. *In* Lyle, M., Koizumi, I., et al., *Proc. ODP, Init. Repts.,* 167: College Station, TX (Ocean Drilling Program).

Sparks, J.W., and Zuleger, E., 1995. Data report: Chemical analyses of the Leg 140 reference sample. *In* Erzinger, J., Becker, K., Dick, H.J.B., Stokking, L.B. (Eds.), *Proc. ODP, Sci. Results,* 137/140: College Station, TX (Ocean Drilling Program), 353–355.

Staudigel, H., 1979. Chemical analyses of inter-laboratory standards. *In* Donnelly, T., Francheteau, J., Bryan, W., Robinson, P., Flower, M., Salisbury, M., et al., *Init. Repts. DSDP,* 51, 52, 53: Washington (U.S. Govt. Printing Office), 1331–1333.

Su, X., 1996. Development of Late Tertiary and Quaternary coccolith assemblages in the Northeast Atlantic. *GEOMAR Rep.,* 48.

Tissot, B.P., and Welte, D.H., 1984. *Petroleum Formation and Occurrence* (2nd ed.): Heidelberg (Springer-Verlag).

Ms 168IR-103

Table 10. Oxide factors used in normalizing elements to 100% and converting elements to oxides.

Element	Oxide/carbonate	Conversion factor
Si	SiO_2	2.139
Ca	$CaO–CaCO_3$	1.399–2.497
Fe	FeO*	1.358
K	K_2O	1.205
Ti	TiO_2	1.668
Al	Al_2O_3	1.889

Note: * = total iron.